

# Core-Log Integrated Formation Evaluation and Application of Flow Unit Concept at Rudies-Sidri Field, Gulf of Suez, Egypt.

Hassan H. Elkady<sup>1</sup>, Ahmed Salah S. Ahmed<sup>2</sup>, M. Fathy Mohamed<sup>1</sup> and Taher M. T. Mostafa<sup>1</sup>

<sup>1</sup> Geology Department, Faculty of Science, Al-Azhar University  
Nasr City, Cairo, Egypt.

<sup>2</sup> Balayim Petroleum Company,  
Nasr City, Cairo, Egypt.

## Abstract

Core-Log integrated formation evaluation was carried out on the investigated area and the resulted petrophysical parameters were used to construct iso-parametric contour maps. Using Winland's model, flow units were identified from the calculation of pore throat radii at the 35 % pore volume (R35). Identifying and quantitatively characterizing flow unit types are the key step in this study because it subdivides the core data samples into units having similar and predictable flow characteristics. In this study, flow unit distribution was scaled up to create new relationships between porosity and permeability and improve permeability prediction using empirically derived model of high correlation coefficients.

**Keywords:** *Core-Log Integration, Formation Evaluation, Petrophysics, Rudies-Sidri Field, Gulf of Suez, Flow Unit.*

## Introduction

The Gulf of Suez Basin is still considered the most prolific and productive petroleum province in Egypt, with the potential to achieve Egypt's goals. It is the location of an extensive hydrocarbon play and has excellent hydrocarbon potential. Rudeis-Sidri Field is located on the eastern coast of the Gulf of Suez (fig. 1), about 25 Km. north of Belayim Land Field, to the South East of October and Ras Budran Fields. A complete set of logs was used to evaluate Nukhul reservoir in the investigated area and the available core data was used for permeability prediction.

## Geologic Setting

The Gulf of Suez is a Neogene continental rift system that developed by the separation of the African and Arabian plates in Late Oligocene – Early Miocene time. Geomorphologically it represents a rejuvenated, slightly arcuate NW-SE topographic depression, known as the Clysmic Gulf (Bosworth and McClay, 2001). Rudies-Sidri field is located in the central part of the Gulf of Suez.

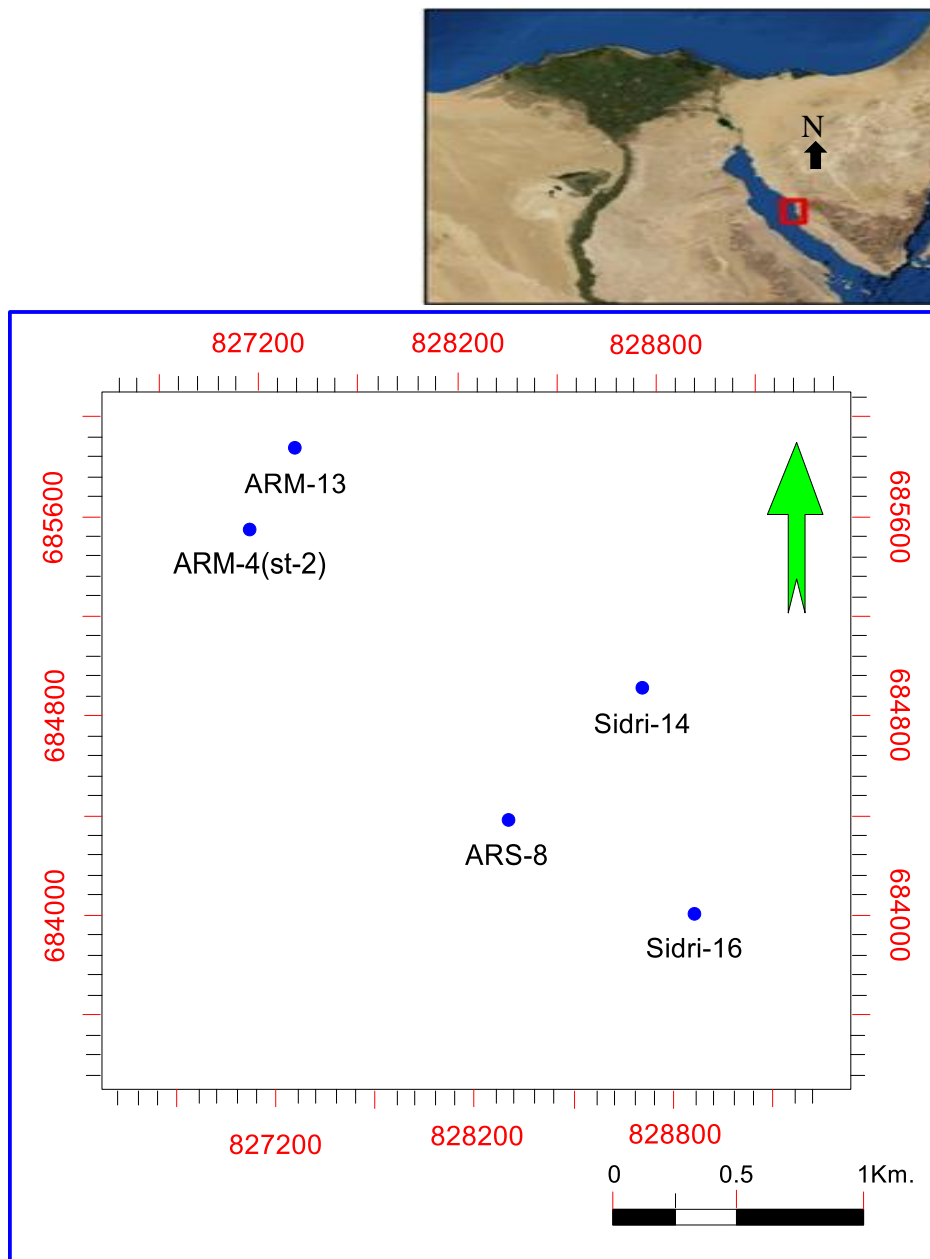


Fig. 1 Location Map of the Study Area Illustrating the Studied Wells.

### Lithostratigraphy

The stratigraphy of the Gulf of Suez can be divided into three major tectono stratigraphic successions (Plaziat et al., 1998) and lithostratigraphic units (Alsharhan, 2003). They comprise:

- I. A pre-rift (pre-Miocene or Palaeozoic–Eocene) succession;
- II. A syn-rift (Oligocene–Miocene) interval (Al- Hussein, 2012; Soliman, et al., 2012; El Atfy et al., 2013a, b); and
- III. A postrift (post-Miocene or Pliocene–Holocene) interval (Alsharhan, 2003).

A generalized stratigraphic column of the Gulf of Suez (fig. 2) modified after Abo Ghonaim, 2014.

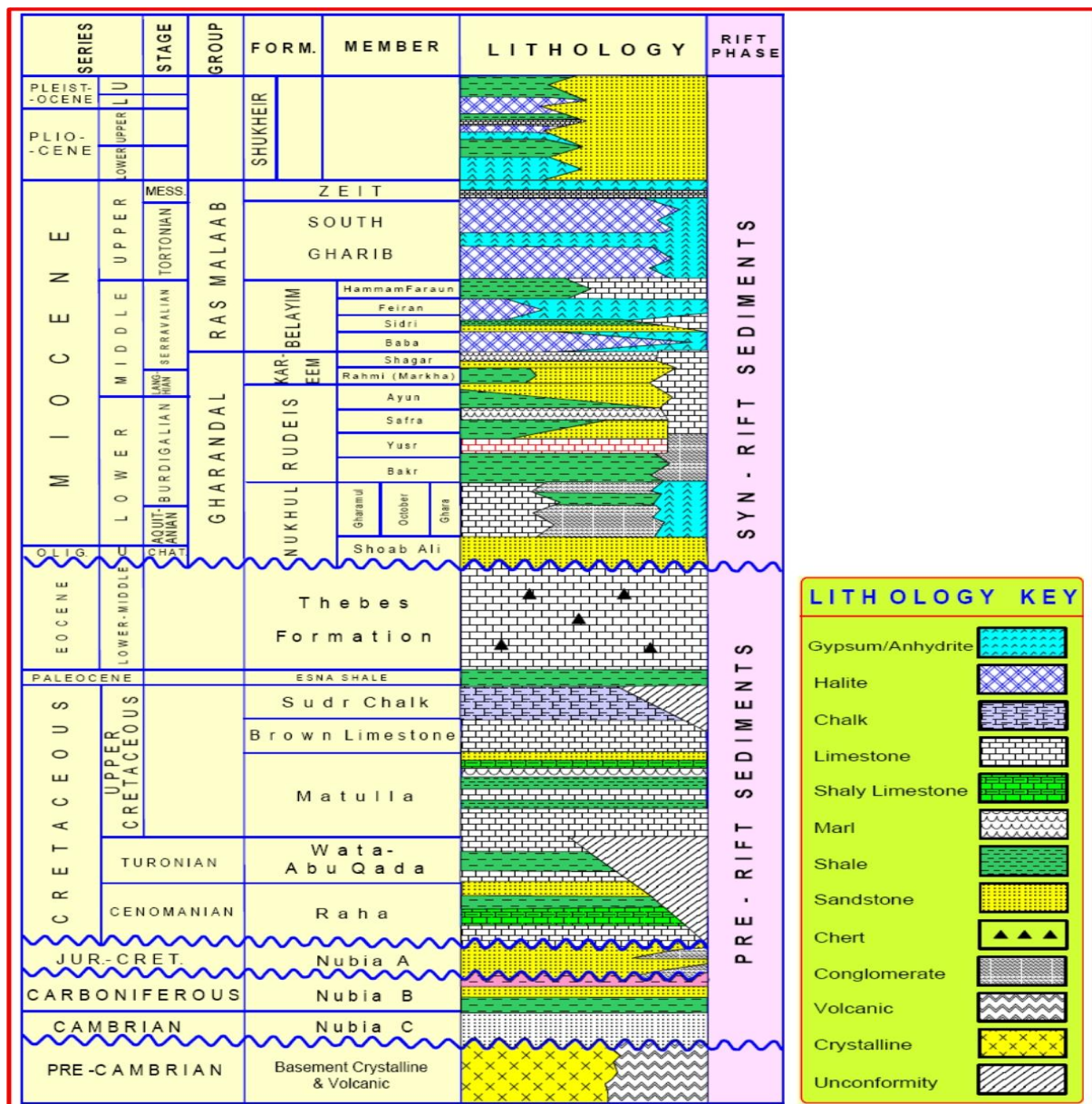


Fig. 2 Generalized Stratigraphic Column of the Gulf of Suez (Modified After Abo Ghonaim, 2014).

The main target of this study, Nukhul formation is located in the syn-rift interval. The Nukhul Formation is the lowermost marine syn-rift unit and unconformably overlies the Eocene Thebes Formation limestone throughout much of the southern Gulf of Suez. The overlying Rudeis Formation is composed of highly fossiliferous shales and marls (referred to as Globigerina marls) and sandstones (Schlumberger, 1984).

### Structural Framework

The Gulf of Suez is dissected by a complex pattern of faults: N-S to NNE-SSW as well as E-W trending normal faults at the rift borders and within the rift basin, and NE-trending strike-slip faults crossing the Gulf basin (Abd El-Naby et al., 2009). The interaction of these major fault systems resulted in a complex structural pattern consisting of numerous horsts and grabens with variable relief and dimensions.

The Gulf of Suez is currently subdivided into three structural provinces according to their structural setting and regional dip directions. (El Diasty et al., 2014)

As implied before, Rudies-Sidri Field is located in the northern part of the central province of the Gulf of Suez so, it is important to focus on the geologic setting of the central province and the following are Geological interpretation of seismic section through the central sector (Fig. 3).

The Central Province occupies the central part of the Gulf of Suez. The characteristic feature of that province is the pre-Miocene shallow structures underlying the Miocene sediments. These highs were subjected to severe erosion. The eroded Pre-Miocene sediments were redeposited in the early troughs such as October and Gharib troughs. The regional dip is north east. The main clysmic and Aqaba trending throw toward the southeast and northwest respectively.

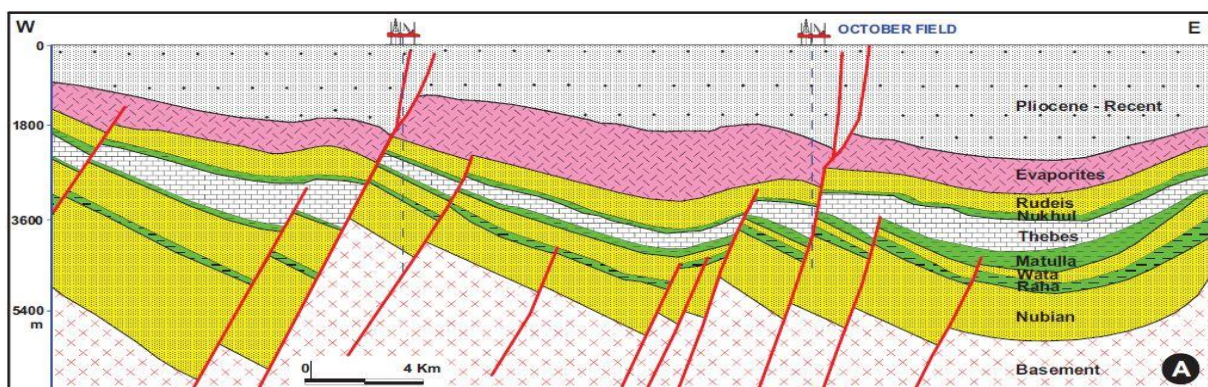


**Fig. 3 Geological - Seismic Section Through the Central Sector of the Gulf of Suez Province (El-Ghamri et al., 2002).**

## Material and Methods

A complete set of log data, including (Gamma ray, Shallow and Deep resistivity, Density and Neutron) in addition to core data were used to evaluate Nukhul formation in the study area and a data set of laboratory measurements porosity, permeability and R35 in sandstone core samples were used in a Permeability prediction technique based on flow unit concept using Winland formula which is:

$$\text{Log R35} = 0.732 + 0.588 \log \text{Kair} - 0.864 \log \phi \text{ core} \quad (1)$$

where **R35** is the pore aperture radius corresponding to the 35th percentile of mercury saturation in a mercury porosimetry test, **Kair** is the uncorrected air permeability (md), and  $\phi$  is porosity (%).

## Formation Evaluation

Using the available log data and core analysis, a complete quantitative well log analysis through Computer Processed Interpretation (CPI) using Interactive Petrophysics (IP) and Techlog programs was accomplished through the following procedures:

## Cutoff and Summations

Shale volume Vsh, Porosity and Water Saturation were used as cutoffs to detect the net pay parameters. Core data was used to determine the cut off values of these parameters. The resulted cutoff values are 8 % for porosity (fig. 4), 30 % of shale volume (fig. 5), and 58 % for water saturation (fig. 6).

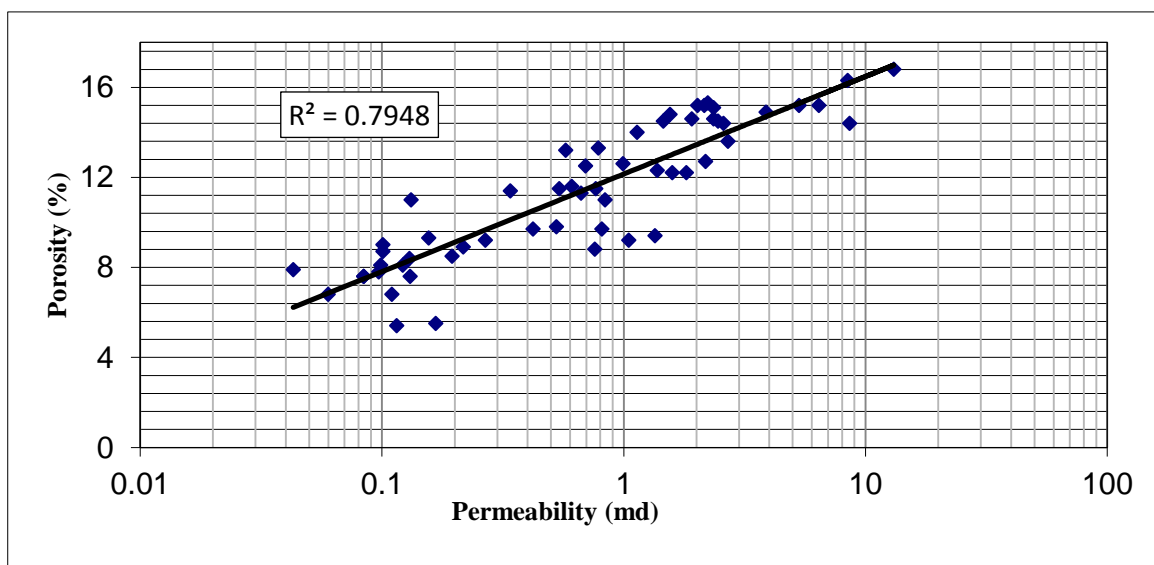


Fig. 4 Porosity Cut off Estimation.

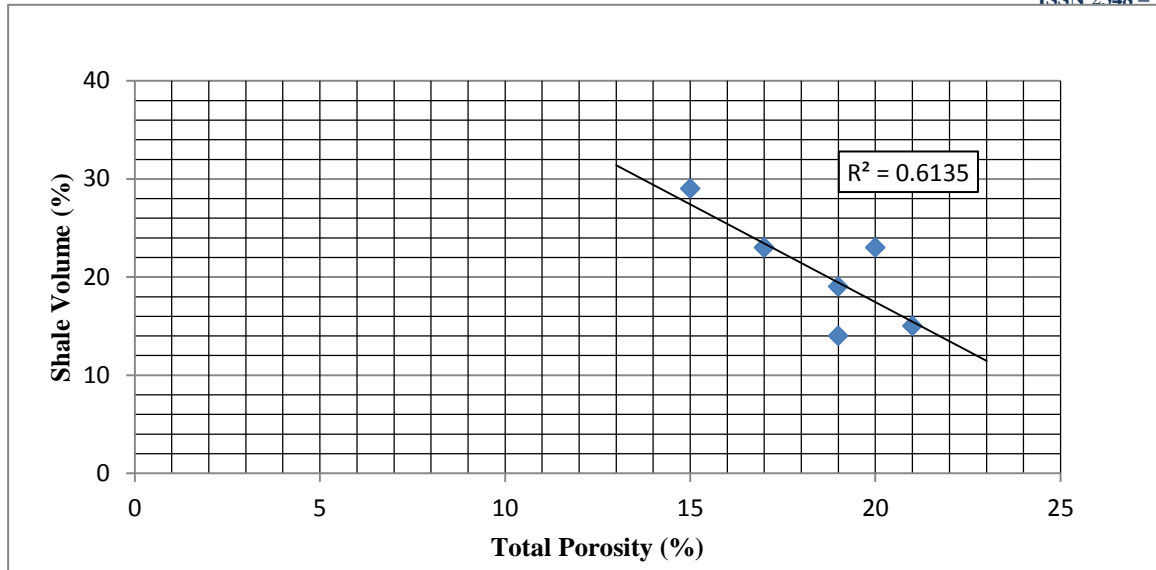


Fig. 5 Shale Volume Cut off Estimation.

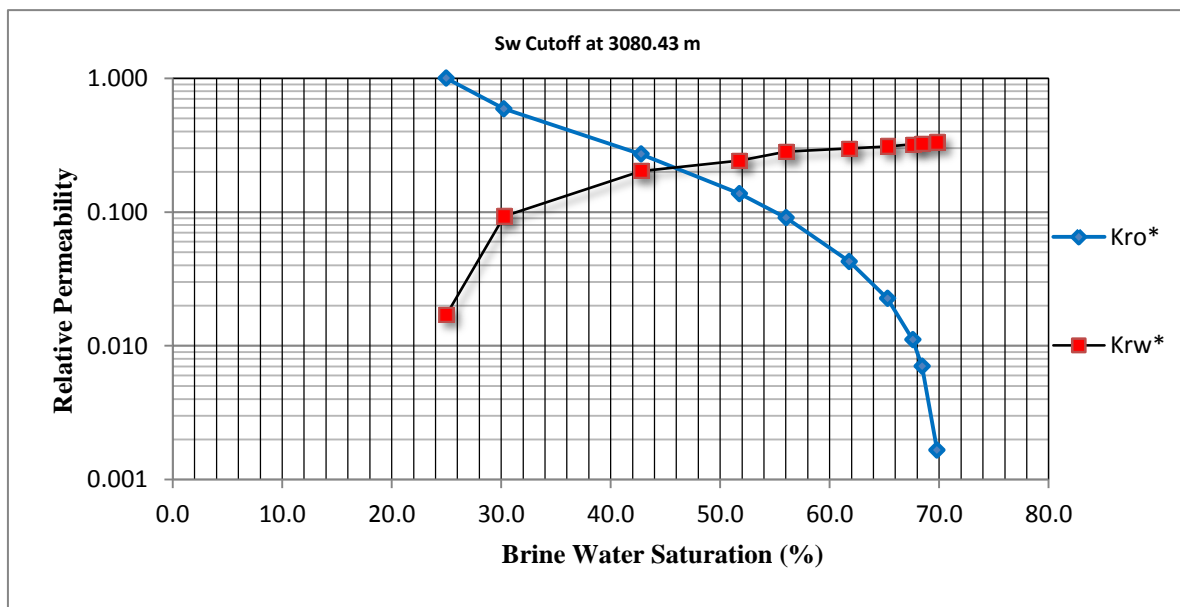
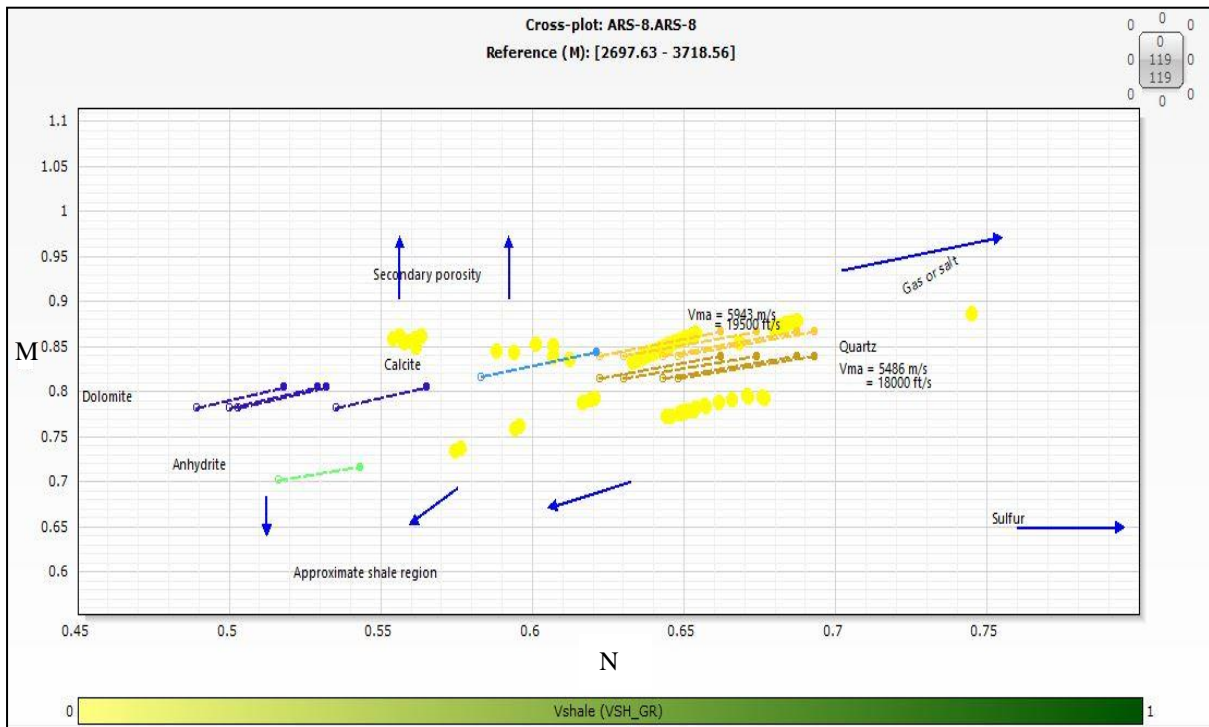


Fig. 6 Water Saturation Cut off Estimation.

## Lithological Identification

Using log data (Density, Neutron and Sonic), Both M-N Cross plot and Dia-porosity Cross plot were constructed to identify the lithological composition of Nukhul formation in the study area. These results were confirmed using core samples thin sections.

It was demonstrated that Nukhul formation composed of sandstone as a matrix and limestone and dolomite as cement with little amounts of k-feldspars and heavy minerals in addition to shale layers within the formation. The mineralogical composition of Nukhul-C is illustrated below figures 7, 8 and 9.



**Fig. 7 M-N Coss Plot of Nukhul-C in Well ARS-8.**

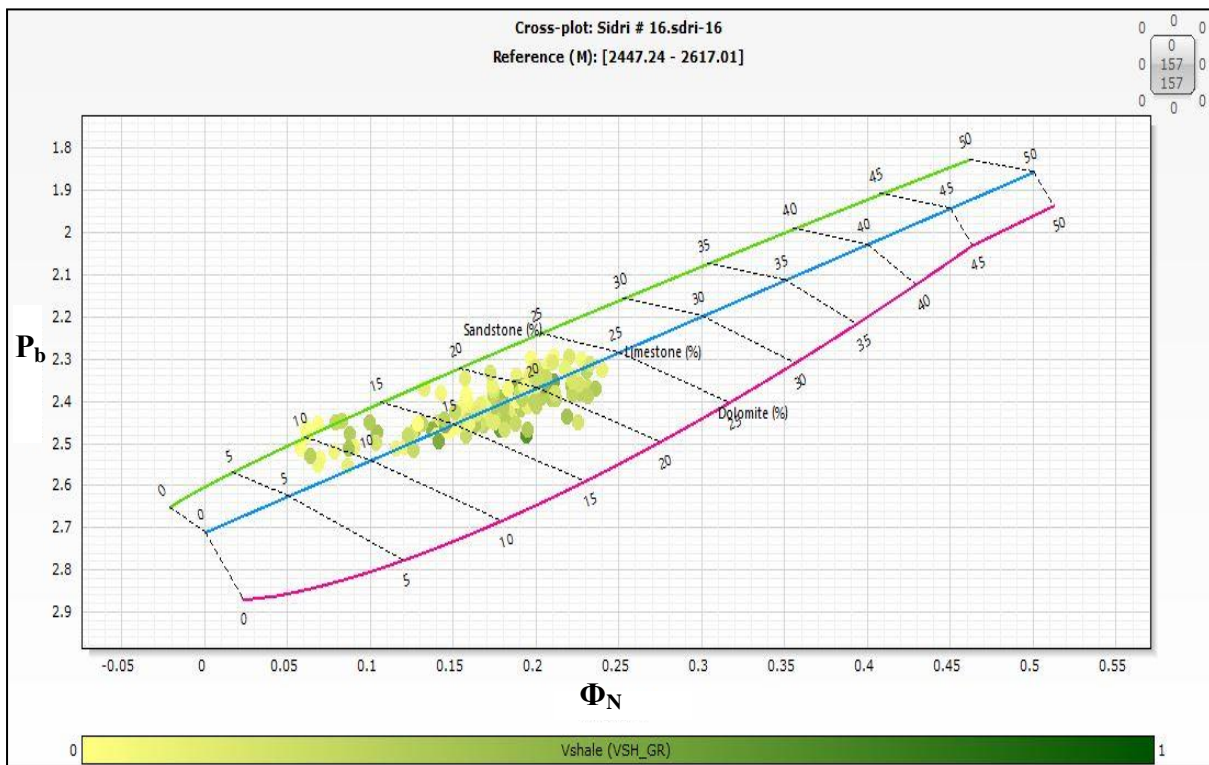


**Fig. 8 Neutron-Density Cross-plot of Nukhul-C in Well Sidri-16.**



**Fig. 9 Mineralogical Composition Thin Section of Nukhul-C (Core Sample).**

### Shale Type Identification

Shale type was identified through IP program and was confirmed by  $\Phi D$  versus  $\Phi N$  plot after Thomas Steiber (1975). It was demonstrated that the shale type in the Nukhul-C is dispersed (fig. 10).

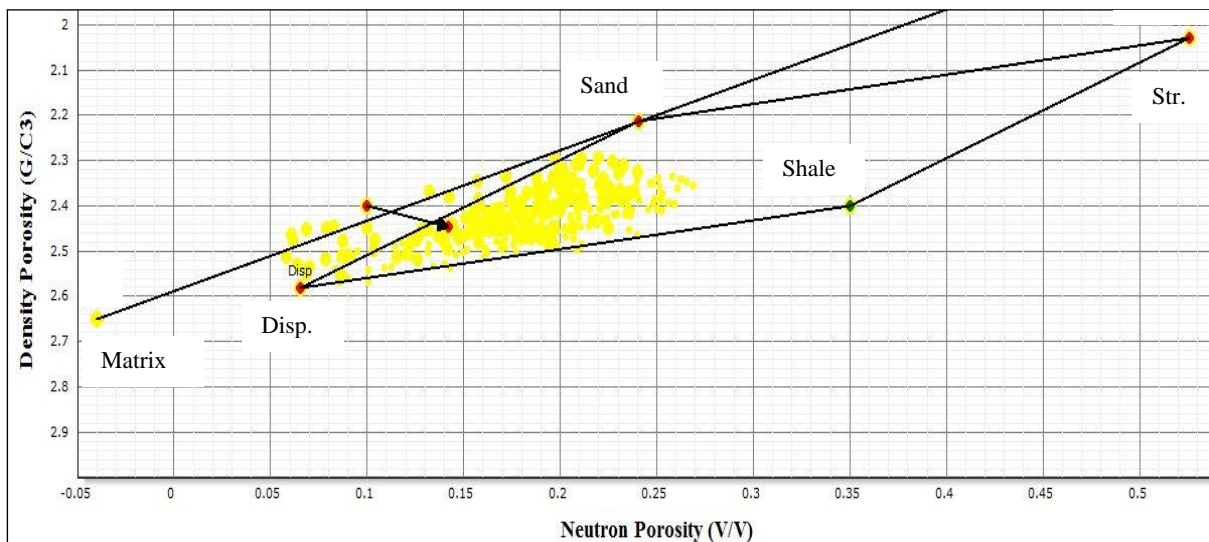


**Fig. 10 Shale Type Identification Through Thomas Steiber Cross plot of Nukhul-C.**

## Shale Volume Calculation

Both single clay indicator and double clay indicator are used to calculate shale volume, Single clay indicator such as GR, Neutron, Resistivity and SP (Self Potential) logs and double clay indicator such as Neutron-Density, Sonic-Density and Neutron-Sonic. In this study GR is used as a single clay indicator and Neutron-Density is used as a double clay indicator. Shale volume, calculated from logs, was corrected using core data including spectral gamma ray and thin sections.

Using core data(Spectral gamma ray and thin sections), it was clear that shale volume estimated from core data is overestimated because core spectral gamma ray indicates that not all recorded gamma ray emits from the Potassium ions, but it dues to the presence of other heavy minerals such as Uranium and Thorium (fig. 11). Also thin sections taken from core samples indicate that even the recorded amount of Potassium does not represent the volume of shale only because of the presence of K-Feldspars in Nukhul-C (fig. 9).

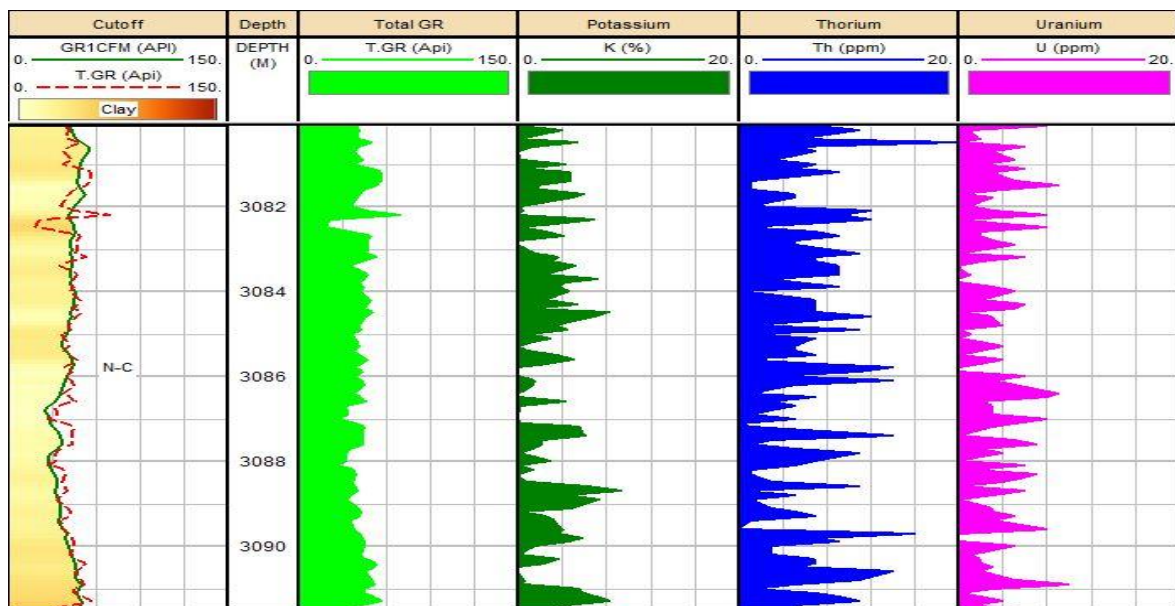
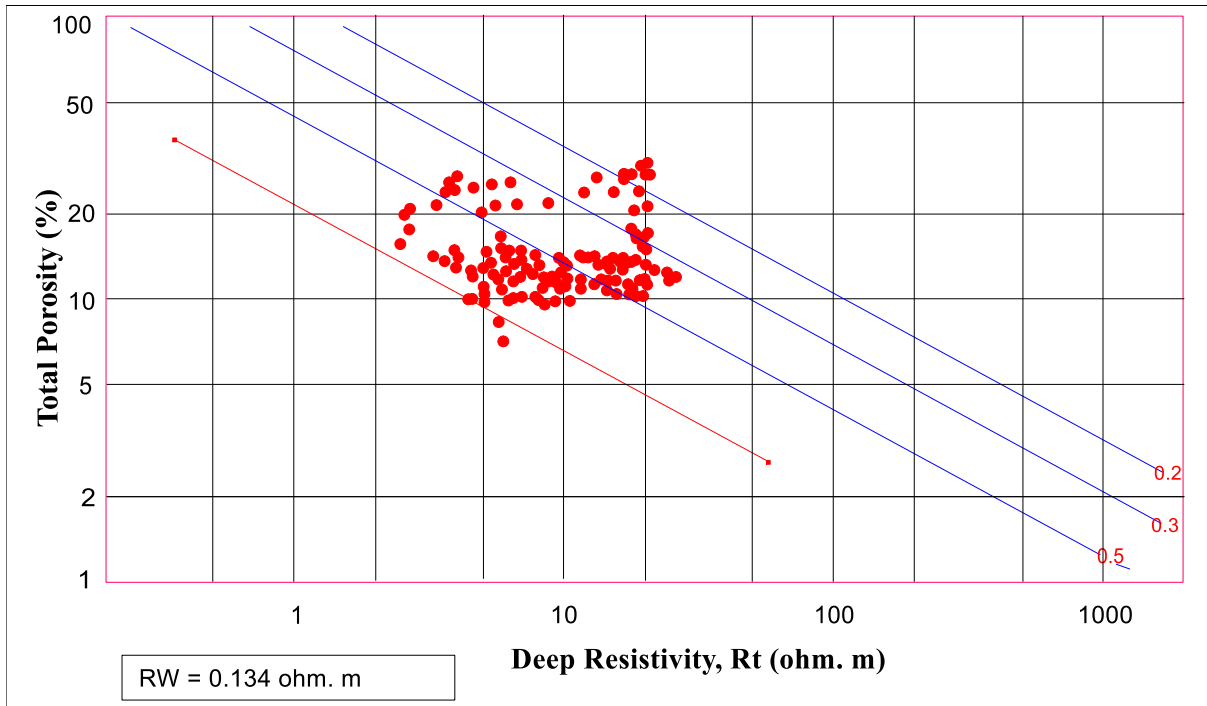


Fig. 11 Spectral Gamma Ray of Core Sample in Nukhul-C.

## Water Resistivity

Water Resistivity ( $R_w$ ) was calculated from Picket Plot. Nukhul-C has two water resistivity values, the first value is about 0.134 ohm. m. and the second value is about 0.14 ohm. m. as illustrated in figures 12 and 13.



**Fig. 12 Picket Plot of Nukhul-C in Well ARS-8.**

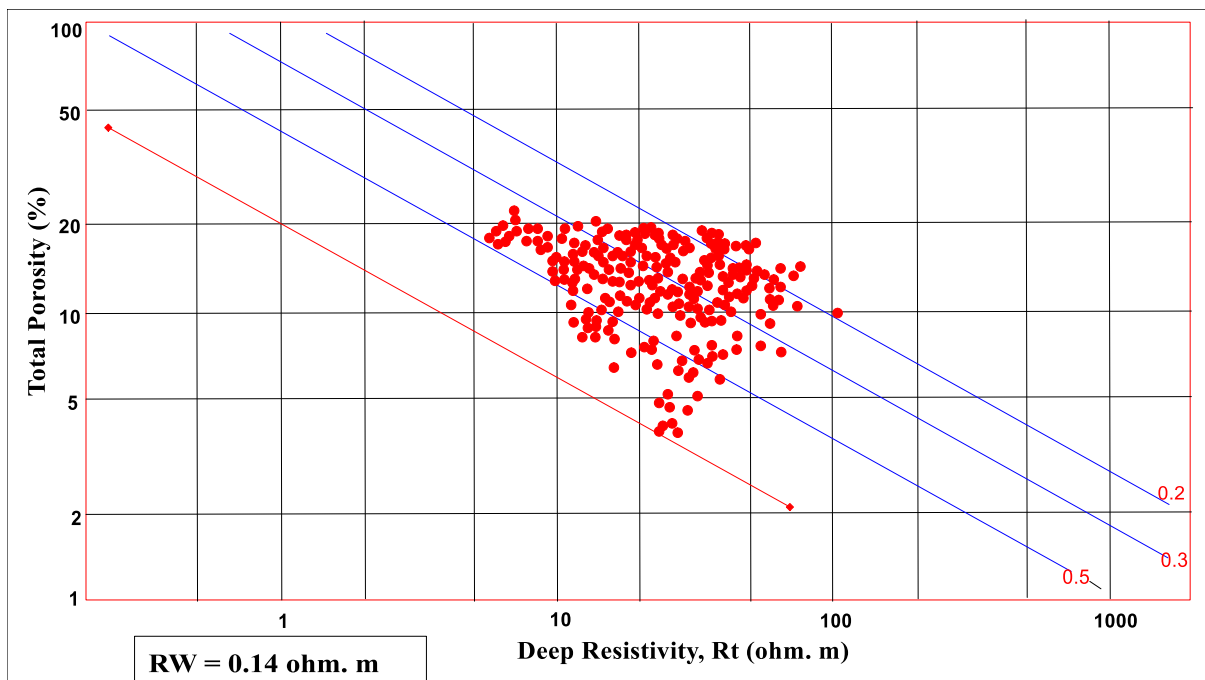


**Fig. 13 Picket Plot of Nukhul-C in Well Sidri-14.**

## Porosity Calculation

Porosity can be calculated using Neutron, Density, Sonic, Neutron logs and/or by combination between any two of them and using Deep Resistivity, Calculated Shale Volume and Estimated Temperature logs.

Measured core porosity was corrected for overburden pressure and uniaxial stress and the resulted porosity was compared with log porosity (fig. 14).

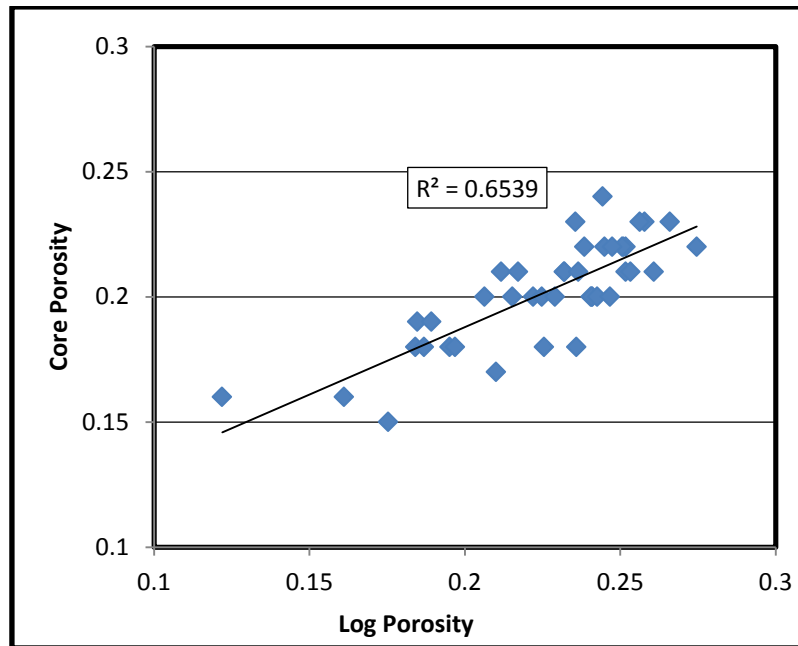


**Fig. 14 Porosity Calculations Using Core and Log Data.**

To calculate Water Saturation (SW), Archie formula is used as a saturation equation using Effective Porosity calculated from neutron-density, shale volume, deep and Shallow Resistivity and calculated water resistivity. The hydrocarbon saturation was determined from water saturation using the following equation:

$$S_h = 1 - S_w \tag{2}$$

### **Illustration of Results and Discussions**

All resulted petrophysical parameters of Nukhul-C are concluded in table 1 and illustrated in two manners, lateral and vertical.

Lateral representation of the resulted petrophysical parameters was accomplished through iso-parametric contour maps of Nukhul-C in the study area. Four iso-parametric contour maps were created to illustrate the lateral distribution of the petrophysical parameters of Nukhul-C (fig. 15).

A vertical representation of the results was created through a computer-processed-interpretation correlation profile A-A\ (fig. 16).

Table 1 Mean Petrophysical Parameters of Nukhul-C.

Well Name	Sidri-14	Sidri-16	Arm-4ST-2	Arm-13	Ars-8
Gross Sand	59 m	24 m	38 m	29 m	28 m
Net Pay	43 m	18 m	23 m	17 m	11 m
Net/Gross	0.7	0.75	0.6	0.6	0.48
Phie	15%	17%	14%	15%	12%
Sw	30%	36%	25%	21%	35%
Shr	70%	64%	75%	79%	65%
Vsh	22%	14%	18%	16%	20%

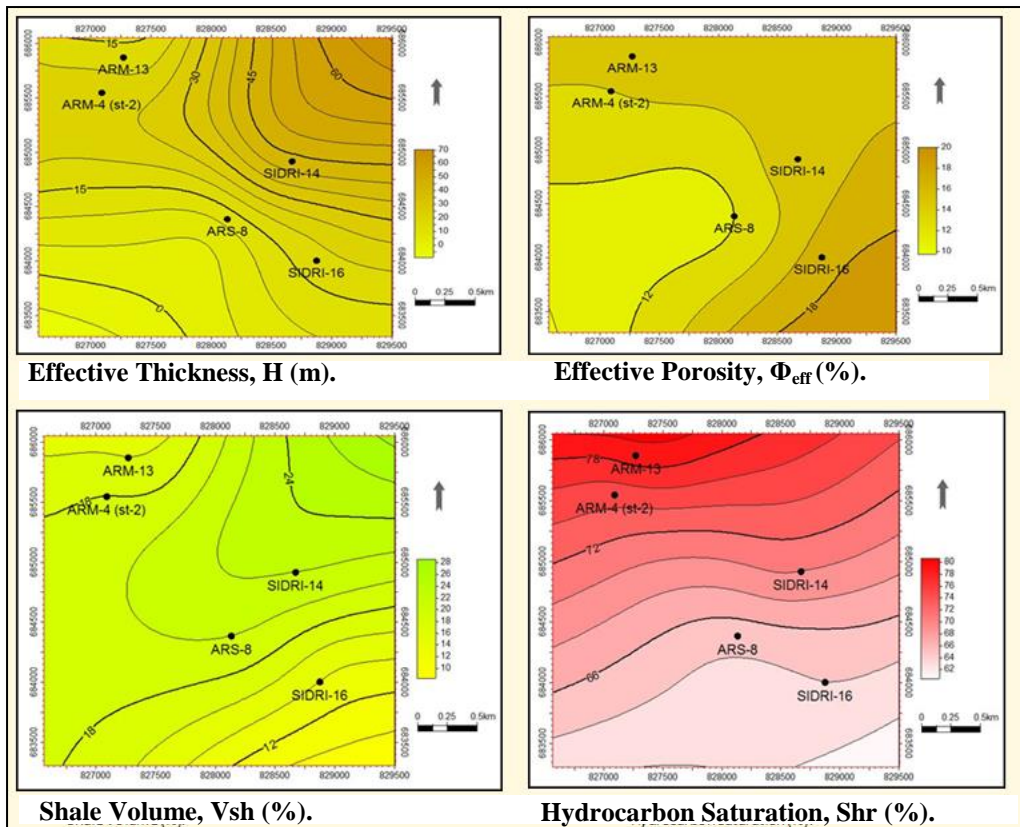
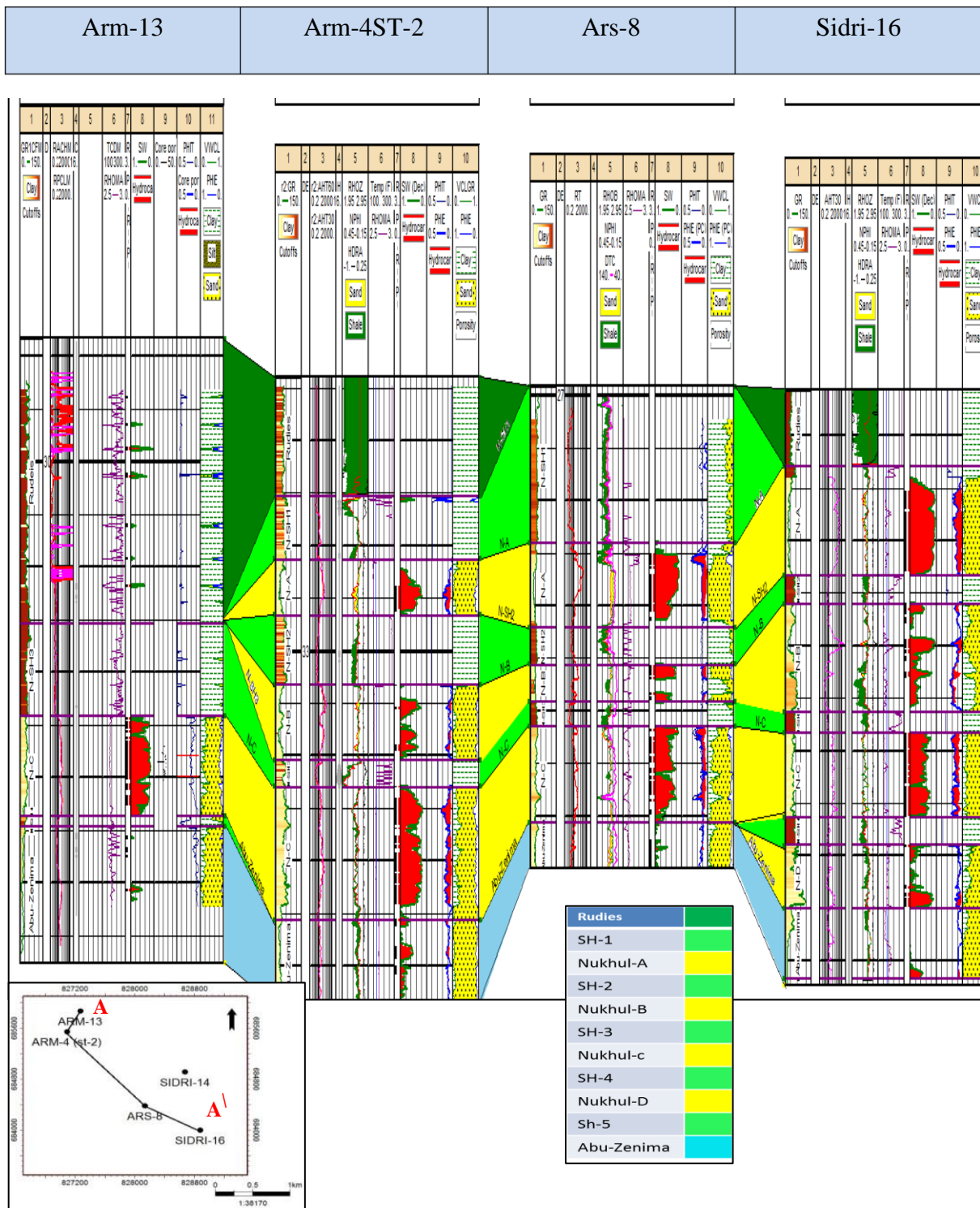


Fig. 15 Iso-Parameters Maps of Nukhul-C.

### Flow Unit Analysis

In this study porosity, permeability and R35 have been measured for all samples in the cored interval (3080m to 3092m) in Arm-13 well. In order to resolve the performance of the studied reservoir formation, we study the effect of petrophysical flow unit types on the relationship between porosity and permeability for all studied core samples and their influence will be distinguished from cross plots and obtained statistical equations.



**Fig. 16 Computer-Processed-Interpretation Correlation along profile A-A'**

Grouping of study core samples is made according to the values of pore throat radius at 35 % of our studied core samples which distinguish each flow unit type and are directly related to the permeability using Winland's model after Pittman, E.D. 1992.

Based on the flow units discrimination illustrated above, three flow units were identified in the cored interval (3080m to 3092m). These three flow units were correlated with log results (fig. 17) and demonstrate a good match between log derived porosity and core measured R35.

Porosity-permeability cross plot was constructed for the three flow unit and a function between the porosity and the permeability was derived for every unit (fig. 18) and can be applied to derive the permeability in other uncored wells.

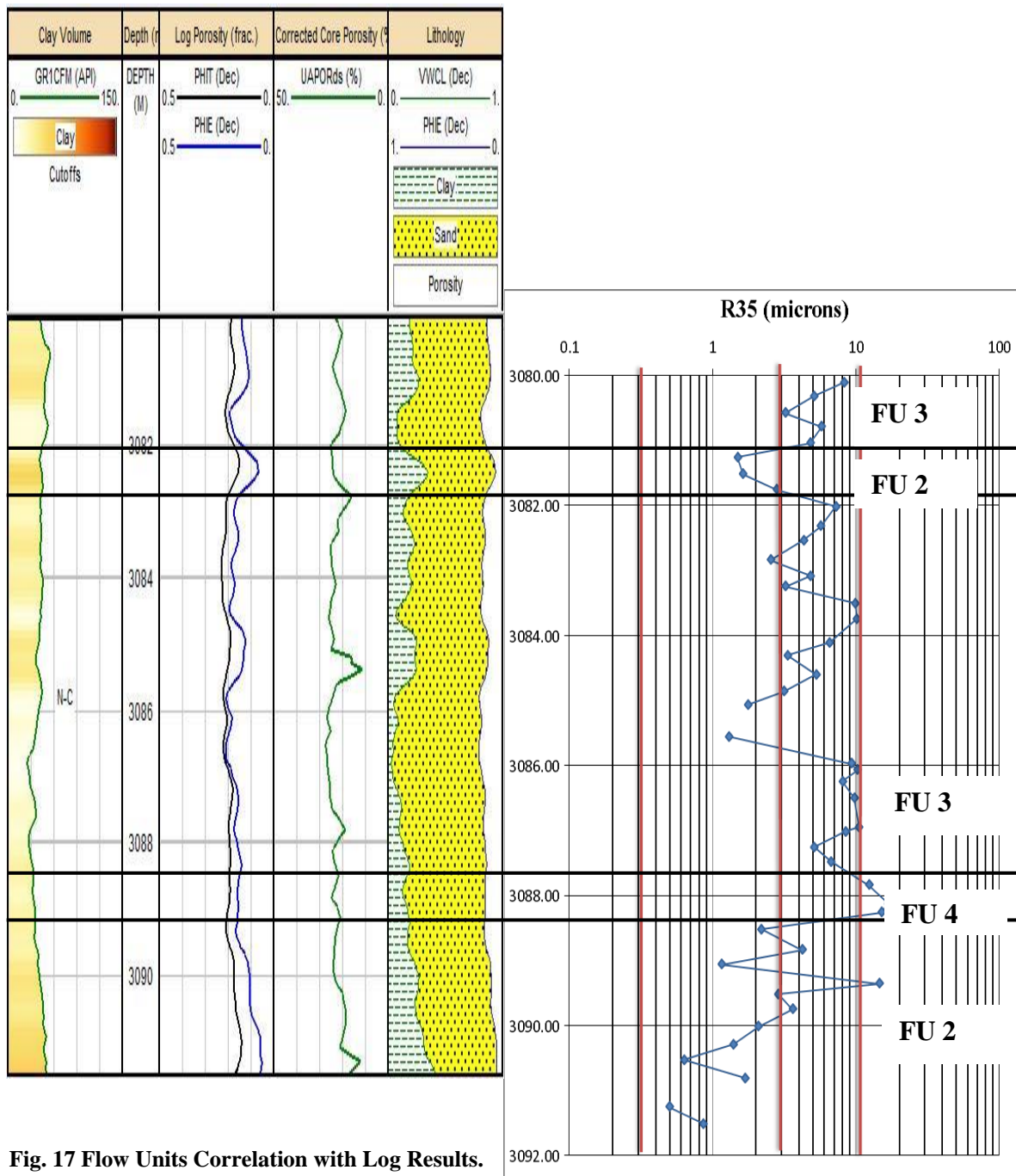


**Fig. 17 Flow Units Correlation with Log Results.**

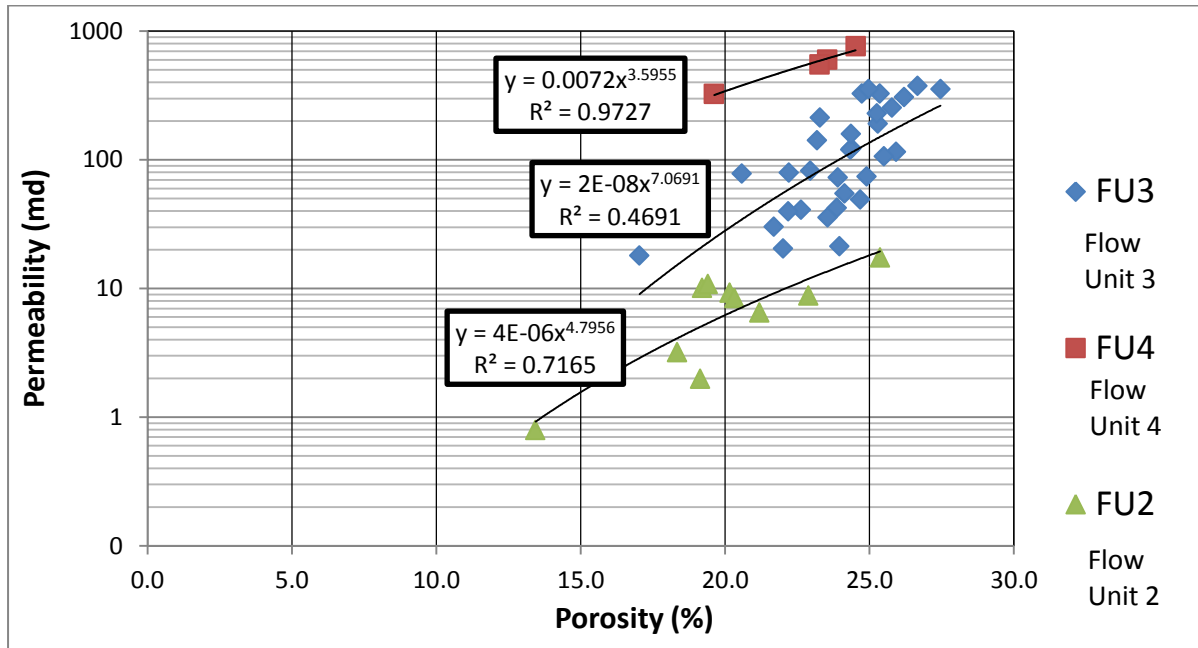


Fig. 18 Flow Unites Porosity-permeability Cross-plot.

### 13-Conclusions

As a result of evaluating reservoir rock in Rudies-Sidri Field through Computer Processed Interpretation (CPI), it can be said that the main reservoir in the investigated area is Nukhul-C.

Nukhul-C consists of Sandstone with Calcite and Dolomite cement and characterized by net pay ranges from 17 m. In Arm-13 well to 43 m. in Sidri-14 well, porosity ranges from 14 % in Arm-4ST-2 to 17 % in Sidri-16 well, Shale Volume ranges from 12 % in Sidri-16 well to 22 % in Sidri-14 well and Hydrocarbon Saturation ranges from 79 % in Arm-13 well to 70 % in Sidri-14 well.

Using flow unit concept, the cored interval in Nukhul-C in Arm-13 well in the study area can be divided into three different flow units according to their measured R35. These flow units when correlated with log results indicated good match.

### References

- Abd El- Naby, A., M. Abd El-Aal, J. Kuss, M. Boukhary and A. Lashin 2009.** Structural and basin evolution in Miocene time, southwestern Gulf of Suez, Egypt. Neues Jahrbuch für Geologie und Paläontologie – Abhandlungen, v. 251, no. 3, p. 331-353.
- Abo Ghonaim, et. al., 2014.** Hydrocarbon Source Rock Evaluation of the Belayim oilfields, Gulf of Suez, Egypt. A thesis submitted to the Department of Geology, Faculty of Science, Mansoura University, Egypt.

- Alsharhan, A.S. (2003).** Petroleum geology and potential hydrocarbon plays in the Gulf of Suez rift basin, Egypt. 'Review American Association of Petroleum Geologists Bulletin, 87 (1), 143-180.
- Bosworth, W. and K. McClay 2001.** Structural and stratigraphic evolution of the Gulf of Suez rift, Egypt: A synthesis. In P.A. Zeigler, W. Cavazza, A.H.F. Robertson and C. Crasquin-Soleau (Eds.), Peri-Tethyan Rift/Wrench Basins and Passive Margins. Mémoire Musée Histoire Naturelle, Peri-Tethys Memoir 6, v. 186, p. 567-606.
- El Atfy, H., Brocke, R. and Uhl, D., 2013a.** Age and Paleoenvironment of the Nukhul Formation, Gulf of Suez, Egypt: Insights from Palynology, Palynofacies and Organic Geochemistry. *GeoArabia*, V. 18, p. 137-174.
- El Atfy, H., Brocke, R. and Uhl, D., 2013b.** A fungal proliferation near the probable Oligocene/Miocene boundary, Nukhul Formation, Gulf of Suez, Egypt. *Journal of Micropalaeontology*, V. 32, p. 183-195.
- El-Ghamri, M., Warburton, I. and Burley, S., 2002.** Hydrocarbon generation and charging in the October Field, Gulf of Suez, Egypt. *Journal of Petroleum Geology*. V. 25, No. 4, p. 433-464.
- Pittman, E.D., 1992.** Relationship of porosity and permeability to various parameters derived from mercury injection-capillary pressure curves for sandstone. *The American Association of Petroleum Geologists bulletin*, 76 (2): 191-198.
- Plaziat, J.C., Montenat, C., Barrier, P., Janin, M.C., Orszag-Sperber, F. and Philobos, E., 1998.** Stratigraphy of the Egyptian syn-rift deposits: correlation between axial and peripheral sequences of the northwestern Red Sea and Gulf of Suez and their relations with tectonics and eustacy. In: Purser, B. H. and Bosence, D. W. J., (Eds.), *Sedimentation and tectonics of rift basins: Red Sea-Gulf of Aden*, p. 211-222.
- Schlumberger, 1984.** In *Geology of Egypt* (pp. 1-64). Paper presented at the Well Evaluation Conference, Schlumberger, Cairo.
- Soliman, A., Ibrahim, M., 2012.** Dinoflagellate cyst stratigraphy and paleoenvironment of the Lower and Middle Miocene, Gulf of Suez, Egypt. *Egyptian Journal of Paleontology*, V. 12, p. a97-122.
- W. Sh. El Diasty and K.E. Peters, 2014.** Genetic classification of oil families in the central and southern sectors of the Gulf of Suez, Egypt, *Journal of Petroleum Geology*, Vol. 37 (2), April 2014, pp 105-126.